

A possible substrate for dopamine-related changes in mood and behavior: Prefrontal and limbic effects of a D3-preferring dopamine agonist

Kevin J. Black^{*†‡§}, Tamara Hershey^{*}, Jonathan M. Koller^{*¶}, Tom O. Videen^{†‡}, Mark A. Mintun^{*‡}, Joseph L. Price^{||}, and Joel S. Perlmutter^{†‡||}

Departments of ^{*}Psychiatry and [†]Neurology and Neurosurgery, [‡]Department of Radiology and Mallinckrodt Institute of Radiology, and ^{||}Department of Anatomy and Neurobiology, School of Medicine, and [¶]School of Engineering, Washington University, 660 South Euclid Avenue, St. Louis, MO 63110

Edited by Marcus E. Raichle, Washington University School of Medicine, St. Louis, MO, and approved November 1, 2002 (received for review May 7, 2002)

Dopamine can induce fascinating, complex human behavioral states, including disinhibition, euphoria, or elaborate stereotypies, whereas dopamine deficiency can cause anxiety or sadness. Limited data suggest that these phenomena may involve dysfunction of orbital frontal cortex, cingulate cortex, or ventral striatum. The dopamine D3 receptor (D3R) has an anatomic distribution that suggests it could mediate these effects, but almost no data directly demonstrate the regional functional effects of D3R activation. We used quantitative positron emission tomography (PET), [¹⁵O]water, and the D3-preferring dopamine agonist pramipexole to identify D3-mediated regional cerebral blood flow (rCBF) responses in living primates. We studied seven normal baboons ventilated with 70% nitrous oxide, and analyzed results voxelwise in a common atlas space. At clinically relevant doses, pramipexole produced statistically robust decreases in rCBF in bilateral orbitofrontal cortex, thalamus, operculum, posterior and anterior (subgenual) cingulate cortex, and insula (in decreasing order of significance). Cortical areas related to movement were relatively unaffected, and rCBF did not change in cerebellum or visual cortex. The dose-response curve and duration of pramipexole's effects suggest that these rCBF responses indicate functional effects of a D3-preferring agonist. A D2-preferring agonist studied under the same conditions produced a quantitatively different pattern of responses. We conclude that a dopamine D3 receptor agonist preferentially affects brain activity in prefrontal and limbic cortex, and speculate that dopamine's effects on these regions via D3Rs may mediate some of the known psychiatric complications of dopamine deficiency or excess.

The neurotransmitter dopamine is important for many normal brain functions, including movement and higher-level functions such as motivation, reward, working memory, and addiction (1–4). Dopamine deficiency leads not only to parkinsonian motor signs but also to anxiety, impaired cognition, or depressed mood (5–7). Conversely, excessive dopaminergic stimulation also causes abnormal emotion and behavior, including euphoria, disinhibition, or repetitive stereotyped movements (7–10). Limited neuroimaging data and lesion studies suggest that dysfunction of orbital frontal cortex, cingulate cortex, or ventral striatum may produce these fascinating phenomena (11, 12).

Given these observations, the discovery of dopamine D3 receptors (D3Rs) and their anatomic localization to brain regions associated with limbic and prefrontal cortex stimulated great scientific interest (13, 14). These regions include ventral pallidum, amygdala, ventral tegmental area, the islands of Calleja, and striatal striosomes (15, 16). This anatomy makes plausible the hypothesis that activating D3Rs may preferentially affect the limbic or prefrontal cortical regions previously implicated in dopamine-influenced complex behavior. However, an agonist applied to a receptor in one brain region (e.g., putamen) can affect neuronal function in remote brain regions (e.g., motor cortex), and no published studies have directly tested which parts of the brain are most affected by activation of D3Rs (17, 18, **).

We have now addressed this question directly, by using positron emission tomography (PET) blood flow measurements and the D3-preferring dopamine agonist pramipexole to measure D3R-mediated effects on regional brain activity. This approach has identified regional effects of other dopamine agonists or levodopa in humans and nonhuman primates (19, 20, ††, 22–25). Such studies reveal changes in regional neuronal (and glial) activity rather than direct vascular effects on blood flow, and are sensitive to important functional changes induced by lesions or treatment (reviewed in refs. 20, 22, and 24). Mapping agonist-induced effects also can identify and prioritize brain regions for future electrophysiological study. The goal of the present study was to determine which areas of the primate brain respond to D3R activation.

Methods

Study Protocol. With the prior approval of the Washington University Animal Studies Committee, we performed nine PET studies in seven normal baboons sedated with 70% inhaled N₂O and 30% O₂. Each study included triplicate measurements of regional cerebral blood flow (rCBF) at baseline and again ≈15–45 min after each of three i.v. doses of pramipexole (5, 50, and 500 μg/kg) for a total of 97 CBF scans (the 5 μg/kg dose was skipped in one study and the 50 μg/kg dose was skipped in another). These doses were chosen to bracket the putative antiparkinsonian dose (see *Pharmacologic Challenge*). Scans were performed in a quiet room with the animal's eyes covered. Using the same protocol, but withholding the dopamine agonist, we performed 48 control rCBF measurements in three baboons. Further details of animal preparation, experimental setup, and the rationale for the choice of sedative are given elsewhere (22).

Pharmacologic Challenge. Pramipexole is a nonergot dopamine agonist with marked selectivity for D2-like (D2, D3, D4) over D1-like receptors and a 5- to 10-fold preference for D3Rs over D2 or D4 receptors (*K_i* reported as D1/D5, >1000 nM; D2, 7.5 nM; D3, 0.9 nM; D4, 9.1 nM; α2-adrenergic, 188 nM) (26–28). Pramipexole is effective in treating parkinsonism and also has antidepressant activity (29). The reported ED₅₀ for antiparkinsonian effect in rhesus monkeys is 45 μg/kg i.m., an observation

This work was presented in part at the Society for Neuroscience Annual Meeting, November 18, 1996, and at the Joint Annual Meeting of the American Neuropsychiatric Association and Behavioral Neurology Society, February 3, 1998.

This paper was submitted directly (Track II) to the PNAS office.

Abbreviations: D3R, dopamine D3 receptor; CBF, cerebral blood flow; rCBF, regional CBF; PET, positron emission tomography; FDG, [¹⁸F]fluorodeoxyglucose.

[§]To whom correspondence should be addressed at: Campus Box 8134, 660 South Euclid Avenue, St. Louis, MO 63110-1093. E-mail: kevin@npg.wustl.edu.

**Camacho-Ochoa, M., Evans, D. L., Walker, E. L., Mattichak, S. & Piercey, M. F. (1994) *Soc. Neurosci. Abstr.* 20, 1355.

††Perlmutter, J. S., Rowe, C. C. & Lich, L. L. (1993) *J. Cereb. Blood Flow Metab.* 13, S286 (abstr.).

that prompted our choice of doses (27). In monkeys, pramipexole inhibited haloperidol-induced dystonia at 116 $\mu\text{g}/\text{kg}$ i.m (30). In rats, 66 $\mu\text{g}/\text{kg}$ i.v. was the ED_{50} for suppression of neuronal firing in dopaminergic neurons in pars compacta of substantia nigra.^{††} For comparison, the recommended daily dose for patients with Parkinson's disease is $\approx 20\text{--}60$ $\mu\text{g}/\text{kg}$. The elimination half-life is ≈ 12 h.

PET Image Acquisition. PET studies were performed on a Siemens (Iselin, NJ) 953B scanner in 2D wobble mode. CBF was measured by using arterial sampling and a 40-s emission scan after the i.v. bolus injection of 20–50 mCi (1 Ci = 37 GBq) ^{15}O -labeled water. This method has been validated and applied in baboons (22, 24, 25, 31–33).

Initial Processing of PET Images. PET images were reconstructed, smoothed to a final resolution of ≈ 8 mm, and transformed to a common atlas space as described (22, 24, 34).

Absolute CBF. Absolute CBF was quantified in all pramipexole studies and two of the control studies, by using arterial blood sampling and published methods (31–33). The brain region used for whole-brain CBF determination was defined by the baboon brain mask image available at <http://purl.org/net/kbmd/b2k>.

Global Glucose Metabolism. One normal baboon was studied twice, 6 wk apart, by using PET and [^{18}F]fluorodeoxyglucose (FDG). Animal preparation, the PET camera, and image reconstruction methods were as described above. For one study, 50 $\mu\text{g}/\text{kg}$ pramipexole was infused i.v., followed 15 min later by i.v. infusion of 10 mCi FDG. Sequential PET images, initially 10 s and increasing to 4 min in length, were acquired for 72 min. Arterial blood was sampled at increasing intervals from 3–4 s at the beginning of the scan to 15 min at the end, and 0.5-cc aliquots were counted in a well counter that had been calibrated to a known source. Serum glucose was measured on arterial samples at 0, 5, and 75 min after FDG injection. The control study used the same protocol, except that pramipexole was not given and the FDG dose was 21 mCi. Tissue activity curves were generated from the same whole-brain region of interest used for whole-brain CBF. The whole-brain metabolic rate of glucose was calculated from these data as (plasma glucose concentration/lumped constant) $\cdot k_1 \cdot k_3 / (k_2 + k_3)$ after numerical estimation of rate constants $k_1 - k_3$ in a tracer kinetic model of FDG metabolism (35). Assumed values were used for k_4 , blood volume fraction, and the lumped constant (36). The kinetic model fit the observed data well, with estimated errors in $k_1 - k_3$ of only 2.9–6.8%.

Statistical Methods. Quantification of CBF using arterial sampling was necessary to test whether pramipexole caused global effects on brain CBF. Quantification was also necessary for physiological interpretation of any regional responses.

However, for regional analysis of the PET data, we wanted to identify brain regions most affected by pramipexole. For this purpose, we used normalized PET counts, which are linearly related within a given scan to rCBF (37). This approach allows us to include more data (because arterial sampling was not possible for some scans) and reduces noise because quantification of absolute CBF includes several additional measurement steps.

All 185,479 voxels within the brain mask were analyzed (≈ 185 ml). At each voxel, we used SPM99 (www.fil.ion.ucl.ac.uk/spm/spm99.html) to fit a general linear model that included an

additive subject effect to account for differences in response between animals. Each scan was included, with the 3 scans at each dose treated as a repeated measure. Because we did not know *a priori* the shape of the dose-rCBF-response curve, the primary contrast for identifying regional responses compared the baseline scans to the scans after the highest dose of pramipexole (500 $\mu\text{g}/\text{kg}$; ref. 24). A drug – baseline or baseline – drug contrast produced a voxelwise test statistic corresponding roughly to a paired *t* test. An initial magnitude threshold corresponding to $P < 0.001$ was applied to this *t* image, and SPM99 then corrected for multiple comparisons by computing the probability that each contiguous cluster of voxels attaining this magnitude would have occurred by chance, given the spatial extent of the activated region. Regional activations were considered significant with a *corrected* probability of $P < 0.05$. This correction has been validated by using simulations (38, 39). Within a significant cluster, we report local maxima of the *t* image that are separated by at least 8 mm (“peaks”). Amplitude and time-course data for selected peaks were computed based on an 8-mm-diameter spherical region of interest centered on the peak coordinate reported by SPM99.

Results

Whole-Brain Effects. Whole-brain mean blood flow decreased in a dose-related fashion after administration of pramipexole (ANOVA, $F_{3,18} = 4.68$, $P < 0.02$). Mean \pm SD blood flow at baseline and after 5, 50, and 500 $\mu\text{g}/\text{kg}$ pramipexole i.v. was 63.5 ± 17.9 , 61.3 ± 17.3 , 48.6 ± 12.8 , and 50.2 ± 23.2 $\text{ml}\cdot\text{min}^{-1}\cdot\text{dl}^{-1}$, respectively, for a maximal change of -23% at the intermediate dose. The most significant change occurred between the 5 $\mu\text{g}/\text{kg}$ dose and the two higher doses (post hoc *t* tests, $P < 0.04$). Global CBF did not decrease in the control studies in which no pramipexole was given. In the animal studied once before and once after 50 $\mu\text{g}/\text{kg}$ pramipexole i.v., whole-brain FDG metabolism decreased by 16%, from 4.96 to 4.16 $\text{mg}\cdot\text{min}^{-1}\cdot\text{dl}^{-1}$.

rCBF. After administration of 500 $\mu\text{g}/\text{kg}$ pramipexole i.v., cerebral blood flow decreased disproportionately, relative to the rest of the brain, in a large contiguous voxel cluster including orbitofrontal and cingulate cortex and thalamus (17,118 voxels, corrected $P \ll 0.0001$; see Table 1 and Fig. 1). Only a few voxels in caudate, putamen, or globus pallidus fell within the activated cluster. In regions of interest centered on peaks in this cluster, there were pharmacologically reasonable dose-response curves, and for each region the largest incremental change in rCBF occurred at the reported antiparkinsonian dose of 50 $\mu\text{g}/\text{kg}$ (Fig. 2). Consistent with the long half-life of pramipexole, these regional CBF decreases after drug did not wane perceptibly over the 45–60 min after administration of pramipexole (Fig. 3).

Two contiguous clusters of *relative* increases in regional CBF were identified (4,445 and 33,873 voxels, each with corrected $P \ll 0.0001$); these clusters included the temporal poles, cerebellum, and visual cortex (Fig. 4). However, absolute regional CBF in these areas showed no change (Fig. 5), indicating that these areas were not truly activated but were simply spared from the widespread CBF decrease induced by pramipexole.

Discussion

The D3-preferring dopamine agonist pramipexole caused significant rCBF changes in orbital frontal cortex, thalamus, cingulate gyrus, and insula. Primary motor cortex was less affected, and there was no change in rCBF in areas, such as visual cortex, that have few dopamine-influenced afferents. These results are consistent with the known efferent connections of D3R-rich brain regions.

Pramipexole may alter neuronal activity in orbital and subgenual cortex through several neuroanatomic pathways. D3Rs

^{††}Piercey, M. F., Smith, M. W., Haadsma-Svensson, S. R. & Hoffman, W. E. (1994) *Soc. Neurosci. Abstr.* 20, abstr. 555.10.

Table 1. Peak responses

Voxel T	Voxel P (unc)	Atlas coordinates			Descriptive region name	$\Delta rCBF$, %
		x	y	z		
7.10	2×10^{-10}	13	36	15	R lateral orbital gyrus	-11.0
6.84	5×10^{-10}	-11	39	16	L lateral orbital gyrus	-8.9
5.75	6×10^{-8}	7	7	15	R thalamus (LP/VLP)	-9.0
5.48	2×10^{-7}	-7	5	8	L thalamus (pulvinar)	-9.0
5.43	2×10^{-7}	22	-1	16	(Posterior) R superior temporal gyrus	-8.3
5.12	9×10^{-7}	-19	4	21	L supramarginal gyrus	-6.0
5.11	10^{-6}	4	6	26	Posterior cingulate	-7.5
5.02	10^{-6}	25	12	9	R insula/superior temporal gyrus	-5.1
4.92	2×10^{-6}	25	21	12	R insula	-7.0
4.89	2×10^{-6}	-4	44	23	(Medial) L superior frontal gyrus	-5.1
4.69	5×10^{-6}	1	32	12	(Subgenual) anterior cingulate gyrus	-7.8

Most significant local maxima (34), separated by >8 mm, in the region identified by SPM as showing a significant decrease in rCBF with 500 $\mu\text{g}/\text{kg}$ pramipexole i.v. after accounting for global effects. Voxel T, the *t* value computed at the given voxel; voxel P (unc), the *P* value corresponding to voxel T (87 d.f.) before correction for multiple comparisons; LP/VLP, lateral posterior nucleus/ventral lateral nucleus, pars postrema; $\Delta rCBF$, mean change in rCBF from baseline in an 8-mm-diameter spherical region centered at the given coordinates.

are concentrated in the rostral ventromedial striatum, including the nucleus accumbens and adjacent parts of the putamen and caudate (16). These neurons send GABAergic fibers to the ventral pallidum and rostral globus pallidus (40). There are also D3Rs in these pallidal areas, possibly on axons of striatal neurons (16). Inhibitory projections from the rostral and ventral pallidum extend to the medial part of the mediodorsal thalamic nucleus (41), which interacts reciprocally with the ventromedial frontal cortex (42). This cortical area projects back to rostral ventromedial striatum (43) to complete a striato-pallido-thalamo-cortical circuit (44). This striatal region also receives afferents from other limbic areas, including amygdala and hippocampus; thus, pramipexole may indirectly influence prefrontal and limbic activity through D3Rs in basal forebrain nuclei or the central nucleus of the amygdala.

The greatest response to pramipexole occurred in orbito-frontal cortex. Case studies since Phineas Gage have linked lesions in orbitofrontal cortex with behavioral disinhibition and loss of social constraint (11, 12). Recent studies suggest that these lesions may disrupt visceral and emotional responses to the environment that help humans predict consequences and make decisions (44–47). Orbitofrontal cortex lesions can also produce a manic syndrome, with euphoria, irritability, agitation, and sleeplessness in addition to disinhibition (reviewed in ref. 48). All these behavioral and emotional changes may also be seen during intoxication with amphetamine or cocaine, or in other hyperdopaminergic states (7–9, 48). We now provide functional anatomic evidence that links these two different observations, and we speculate that behavioral disinhibition observed with dopaminomimetic agents may be mediated in part by an inhibitory influence of D3R activation on orbitofrontal cortex.

Similarly, either stimulant drugs or dopaminomimetic treatment for Parkinson's disease can cause repetitive, senseless, complex behavior referred to as "punding" (10). This behavior may be analogous to the stereotypies that stimulants can cause in rodents. In humans, orbitofrontal insults can cause senseless complex movements, including automatic imitation of others' actions (12). Punding also resembles, to a degree, the repetitive complex behavior of obsessive-compulsive disorder. In this disorder, there is excessive orbitofrontal metabolism that is reduced by successful treatment with either medications or

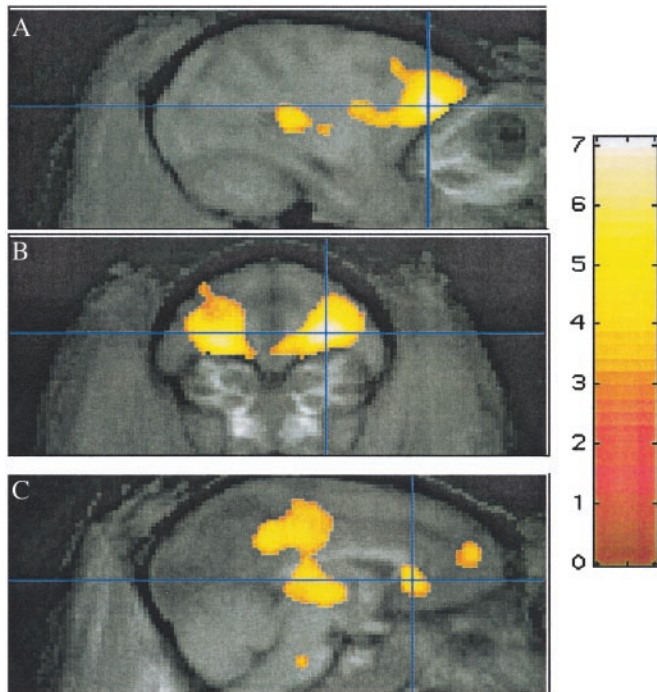


Fig. 1. Selected focal decreases observed after 500 $\mu\text{g}/\text{kg}$ pramipexole i.v. (*t* map in color overlaid on atlas image in grayscale). (A and B) Crosshairs at most significant decrease, atlas (13, 36, 15). (C) Cingulate cortex, atlas (1, 32, 12).

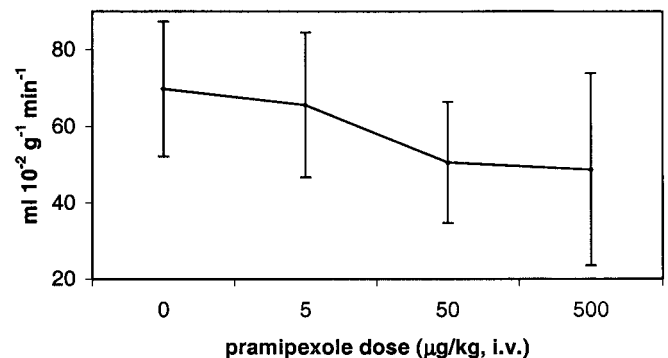


Fig. 2. rCBF, right orbitofrontal prefrontal cortex. Dose-response curve for a region of interest centered at atlas (13, 36, 15), the voxel with the most significant rCBF decrease after 500 $\mu\text{g}/\text{kg}$ pramipexole i.v. (mean \pm SD).

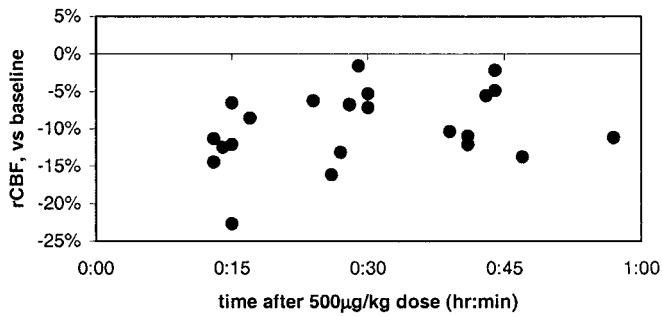


Fig. 3. Change in regional CBF over time, region of maximal decrease (prefrontal cortex). Regional CBF changes after 500 µg/kg pramipexole i.v. persist over the time interval observed. Each point corresponds to one PET scan. Data are from the region of interest described in Fig. 1 A and B and Fig. 2.

behavior therapy (49). Based on these observations and our results, we posit that dopaminergic effects on orbitofrontal cortex via D3Rs may in part cause punding and other complex dopamine-induced stereotypies.

The cingulate cortex response to pramipexole (Fig. 1C) may provide a functional basis for studies linking anxiety and depression with dopamine (7, 8, 29, 48, 50–52) and cingulate cortex (53–55). Patients with major depression have decreased rCBF, metabolism, and volume of subgenual anterior cingulate cortex (54, 56), and postmortem studies in depressed patients show loss of glia in this region (57). Anterior cingulate cortex is innervated by thalamic neurons that are influenced by ventral striatum (58, 59), and dopamine release in the D3R-rich ventral striatum correlates with amphetamine-induced euphoria (60). Major depression and transient sadness in normal volunteers also affect metabolism in the posterior portion of cingulate cortex (53, 54). Levodopa-induced rCBF responses in posterior cingulate are abnormal in a mood disorder that is clearly related to dopamine, namely dose-related mood fluctuations in Parkinson's disease (7, §§). D3 or other D2-like receptors may mediate this abnormal response, because levodopa causes a decrease in posterior cingulate rCBF in baboons as well as people, and pramipexole, but not a D1 agonist, replicates this effect (24, 25). Given these relationships, D3Rs in neuronal circuits that innervate cingulate cortex may mediate, at least in part, known dopaminergic effects on mood.

Regarding the other significant regional activations, the thalamus can be directly or indirectly affected by dopamine, and various thalamic nuclei participate in cortical-striatal circuits (12). Therefore it is not surprising that a dopamine agonist alters flow in the thalamus. However, it would be interesting to determine whether Parkinson's disease patients with treatment-induced dyskinesias, who have an altered thalamic blood flow response to levodopa (23), also have an abnormal thalamic response to this D3-preferring dopamine agonist. Other neuroimaging studies have demonstrated dopaminergic influences on superior temporal gyrus (reviewed in ref. 24).

Striatal and pallidal neurons are presumably involved in mediating the cortical and thalamic responses to pramipexole, and it may at first seem curious that our analysis did not identify peak changes within these nuclei. However, there are several likely explanations. We might not expect to see changes in striatal blood flow, because altered neuronal firing correlates better with metabolic changes observed in axon termini than in cell bodies (62–64). Second, partial volume averaging disproportionately reduces the peak magnitude of the PET signal in

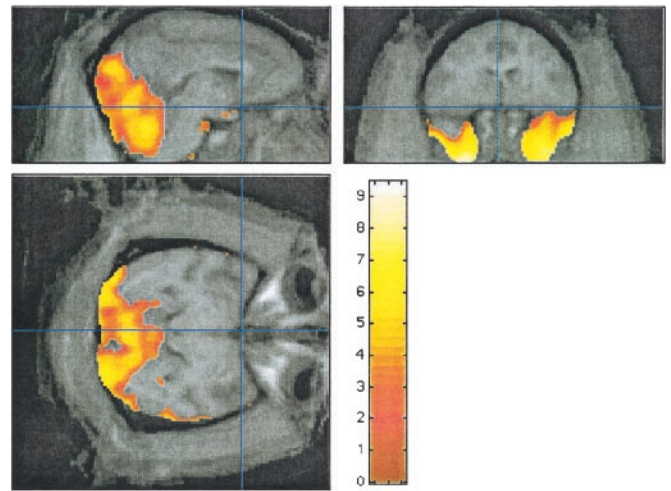


Fig. 4. Relative rCBF “increases” after 500 µg/kg pramipexole i.v. as identified by SPM99 (*t* map in color overlaid on atlas image in grayscale).

small regions. For instance, the external segment of globus pallidus is small relative to the resolution of PET, and rCBF changes in this nucleus could be overshadowed by changes in nearby structures. Parenthetically, most human brain mapping PET studies have been done at image resolutions that raise similar issues. Third, we studied normal animals; in rodent studies, the subcortical responses to DA agonists are much smaller in magnitude in normal animals than in lesioned animals. Alternatively, a larger sample might be required to demonstrate statistical significance in these nuclei.

Our results highlight a methodological strength of this study. Many functional neuroimaging studies use techniques that do not permit quantitative measurements, but rely on qualitative analyses for describing regional changes in CBF. Qualitative analysis is appropriate when there is no global shift in blood flow, but pramipexole substantially affects average brain CBF and renders that simplification inappropriate. If we had used qualitative methods, we might have concluded erroneously that the apparent regional “increases” identified by SPM99 (Fig. 4) represented areas of maximal brain response to pramipexole when in fact they represent areas of minimal response (Fig. 5). Only a quantitative approach, involving arterial sampling, allowed correct identification of regional responses. Another advantage of quantitative methods is that the global effects of pramipexole may themselves be of interest, because sedatives often cause

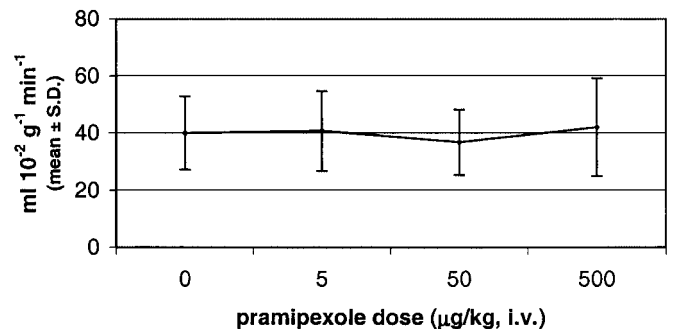


Fig. 5. Absolute rCBF at peak relative “increase.” The relative increases in rCBF after 500 µg/kg pramipexole i.v. are actually regions protected from the widespread decrease in rCBF. Data are from an 8-mm-diameter spherical region centered at the peak relative increase.

⁵⁵Black, K. J., Hershey, T., Hartlein, J. M., Carl, J. L. & Perlmutter, J. S. (2001) *Mov. Disord.* 16, 556 (abstr.).

global decreases in brain metabolism (65) and dopaminergic therapy can cause sleepiness (66–68).

Aside from quantification, another virtue of rCBF PET is the ability to simultaneously survey the entire living brain for areas most sensitive to pramipexole. However, this neuroimaging technique has limitations and cannot address other crucial questions. For instance, decreased regional metabolism and blood flow may reflect decreased firing either of inhibitory or of excitatory neurons (64, 69), or a change in firing pattern such as reduced bursting (21). Furthermore, sedation needed for these baboon studies may change the sign of rCBF responses to dopamine agonists (25). Therefore, from our study alone, we cannot identify the electrophysiological mechanisms underlying pramipexole's effects, but we can confidently identify regional responses to pramipexole (as listed in Table 1). Thus, our neuroimaging approach identifies the functional anatomy needed to guide subsequent physiological investigations. Several of the brain regions we identified have been heretofore studied only sparingly in regards to dopamine-mediated brain function.

The specificity and generalizability of our results are limited by the choice of drug and species. Pramipexole (like all other known D3R preferring dopamine agonists) has limited selectivity for the D3R compared with the D2 receptor (26). To address this point, we reanalyzed data obtained with the same methods in the same seven baboons, using the relatively D2-selective agonist U91356a (22, 26). This drug has K_i of D1, >1000 nM; D2, 1.3 nM; D3, 32 nM; D4, 195 nM; and serotonin 5HT1A, 58 nM; so that the D2:D3 ratio is 1:25, or 200-fold lower than pramipexole's 8:1 ratio (61). In monkeys, the antiparkinsonian dose of U91356a is 10–30 $\mu\text{g}/\text{kg}/\text{day}$ s.c., and the ED_{50} in rats for inhibition of substantia nigra dopaminergic neurons is 32 $\mu\text{g}/\text{kg}$ i.v.^{***†††} Comparing doses of two drugs is difficult, but, in both these models, U91356a is more potent than pramipexole. We used U91356a doses of 1–2 $\mu\text{g}/\text{kg}$, 10–22 $\mu\text{g}/\text{kg}$ (intended to approximate the antiparkinsonian dose), and 100–220 $\mu\text{g}/\text{kg}$ i.v. At the 100–220 $\mu\text{g}/\text{kg}$ dose, the three most significant rCBF decreases are in thalamus, medial parietal cortex, and thalamus (not prefrontal cortex). The dose-response curves in orbital cortex show pramipexole to be more potent at depressing rCBF, although specificity is lost at higher doses (Fig. 6). It seems that, at antiparkinsonian doses, orbitofrontal cortex is much more sensitive to pramipexole than to a D2-preferring agonist, suggesting

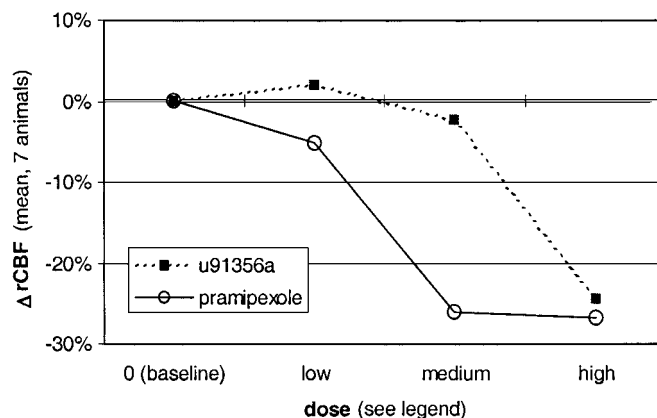


Fig. 6. Change in rCBF at three dose levels of a D3-preferring agonist (pramipexole, open circles and solid line) and a D2-preferring agonist (U91356a, filled squares and dashed line). Pramipexole doses were 5, 50, and 500 $\mu\text{g}/\text{kg}$, and U91356a doses were 1–2, 10–22, and 100–220 $\mu\text{g}/\text{kg}$. For both drugs, the doses were chosen *a priori* so that the intermediate dose approximated the reported antiparkinsonian dose in monkeys.

that the response in orbital frontal cortex is mediated at least in large part by D3Rs.

Pramipexole was not available for human use when this study began. Pharmacologic activation imaging in nonhuman primates with selective experimental drugs like pramipexole may help clarify the human pharmacology of functional responses to approved drugs like levodopa. Having defined the quantitative regional effects of pramipexole in this primate model, future studies may focus on human conditions with hypothesized abnormalities in dopaminergic function, such as drug abuse, schizophrenia, dystonia, or Tourette syndrome.

For technical support, we thank T. Anderson, J. Carl, C. Collins, J. Hood, Jr., B. Tobben, and V. Tolia. For glucose determinations, we thank M. LaRegina. For helpful discussions, we thank M. F. Piercey (since deceased) and P. J. Bédard. Pramipexole was a gift from Upjohn. This work was supported by the National Institute of Neurological Disorders and Stroke (Grants NS01898 and NS41248), the National Alliance for Research on Schizophrenia and Depression, the Tourette Syndrome Association, the Charles A. Dana Foundation, the American Parkinson Disease Association, the Sam and Barbara Murphy Fund, and the McDonnell Center for Higher Brain Function.

^{†††}Piercey, M. F., Moon, M. W., Hoffmann, W. E., Walters, R., Blanchet, P. J. & Bedard, P. J. (1992) *Soc. Neurosci. Abstr.* **18**, 1081.

- Cloninger, C. R. (1987) *Arch. Gen. Psychiatry* **44**, 573–588.
- Caine, S. B. & Koob, G. F. (1993) *Science* **260**, 1814–1816.
- Jackson, D. M. & Westlind-Danielsson, A. (1994) *Pharmacol. Ther.* **64**, 291–369.
- Schultz, W. (1997) *Curr. Opin. Neurobiol.* **7**, 191–197.
- Levin, B. E. & Katzen, H. L. (1995) in *Behavioral Neurology of Movement Disorders: Advances in Neurology*, eds. Weiner, W. J. & Lang, A. E. (Raven, New York), Vol. 65, pp. 85–95.
- Farber, N. B. & Black, K. J. (1997) in *Washington University Adult Psychiatry*, ed. Guze, S. B. (Mosby, St. Louis), pp. 407–426.
- Racette, B. A., Hartlein, J. M., Hershey, T., Mink, J. W., Perlmutter, J. S. & Black, K. J. (2002) *J. Neuropsychiatr. Clin. Neurosci.* **14**, 438–442.
- Goodwin, F. K. (1971) *J. Am. Med. Assoc.* **218**, 1915–1920.
- Brunner, H. G., Nelen, M., Breakefield, X. O., Ropers, H. H. & van Oost, B. A. (1993) *Science* **262**, 578–580.
- Fernandez, H. H. & Friedman, J. H. (1999) *Mov. Disord.* **14**, 836–838.
- Damasio, H., Grabowski, T., Frank, R., Galaburda, A. M. & Damasio, A. R. (1994) *Science* **264**, 1102–1105.
- Mega, M. S. & Cummings, J. L. (1994) *J. Neuropsychiatr. Clin. Neurosci.* **6**, 358–370.
- Sokoloff, P., Giros, B., Martres, M. P., Bouthenet, M. L. & Schwartz, J. C. (1990) *Nature* **347**, 146–151.
- Schwartz, J.-C., Levesque, D., Martres, M.-P. & Sokoloff, P. (1993) *Clin. Neuropharmacol.* **16**, 295–314.

- Sokoloff, P., Giros, B., Martres, M. P., Andrieux, M., Besancon, R., Pilon, C., Bouthenet, M. L., Souil, E. & Schwartz, J. C. (1992) *Arzneimittelforschung* **42**, 224–230.
- Murray, A. M., Ryoo, H. L., Gurevich, E. & Joyce, J. N. (1994) *Proc. Natl. Acad. Sci. USA* **91**, 11271–11275.
- Carta, A. R., Gerfen, C. R. & Steiner, H. (2000) *Neuroreport* **11**, 2395–2399.
- Carta, A. R. & Gerfen, C. R. (1999) *Neuroscience* **90**, 1021–1029.
- Perlmutter, J. S. & Moerlein, S. M. (1999) *Q. J. Nucl. Med.* **43**, 140–154.
- Herscovitch, P. (2001) *J. Clin. Pharmacol.* **41**, 11S–20S.
- Almeida, R. & Stetter, M. (2002) *Neuroimage* **17**, 1065–1079.
- Black, K. J., Gado, M. H. & Perlmutter, J. S. (1997) *J. Neurosci.* **17**, 3168–3177.
- Hershey, T., Black, K. J., Stambuk, M. K., Carl, J. L., McGee-Minnich, L. A. & Perlmutter, J. S. (1998) *Proc. Natl. Acad. Sci. USA* **95**, 12016–12021.
- Black, K. J., Hershey, T., Gado, M. H. & Perlmutter, J. S. (2000) *J. Neurophysiol.* **84**, 549–557.
- Hershey, T., Black, K. J., Carl, J. L. & Perlmutter, J. S. (2000) *Exp. Neurol.* **166**, 342–349.
- Mierau, J., Schneider, F. J., Ensinger, H. A., Hio, C. L., Lajiness, M. E. & Huff, R. M. (1995) *Eur. J. Pharmacol.* **290**, 29–36.
- Mierau, J. (1995) *Clin. Neuropharmacol.* **18**, S195–S206.
- Piercey, M. F. (1998) *Clin. Neuropharmacol.* **21**, 141–151.
- Corrigan, M. H., Denahan, A. Q., Wright, C. E., Ragual, R. J. & Evans, D. L. (2000) *Depress. Anxiety* **11**, 58–65.
- Mierau, J. & Schingnitz, G. (1992) *Eur. J. Pharmacol.* **215**, 161–170.

31. Herscovitch, P., Markham, J. & Raichle, M. (1983) *J. Nucl. Med.* **24**, 782–789.
32. Raichle, M., Martin, W., Herscovitch, P., Mintun, M. & Markham, J. (1983) *J. Nucl. Med.* **24**, 790–798.
33. Videen, T. O., Perlmutter, J. S., Herscovitch, P. & Raichle, M. E. (1987) *J. Cereb. Blood Flow Metab.* **7**, 513–516.
34. Black, K. J., Snyder, A. Z., Koller, J. M., Gado, M. H. & Perlmutter, J. S. (2001) *Neuroimage* **14**, 736–743.
35. Huang, S.-C., Phelps, M. E., Hoffman, E. J., Sideris, K., Selin, C. J. & Kuhl, D. E. (1980) *Am. J. Physiol.* **238**, E69–E82.
36. Hawkins, R. A., Phelps, M. E. & Huang, S.-C. (1986) *J. Cereb. Blood Flow Metab.* **6**, 170–183.
37. Fox, P. T. & Mintun, M. A. (1989) *J. Nucl. Med.* **30**, 141–149.
38. Friston, K. J., Worsley, K. J., Frackowiak, R. S. J., Mazziotta, J. C. & Evans, A. C. (1994) *Hum. Brain Mapp.* **1**, 214–220.
39. Friston, K. J., Holmes, A. P., Poline, J.-B., Price, C. J. & Frith, C. D. (1996) *Neuroimage* **4**, 223–235.
40. Haber, S. N., Kunishio, K., Mizobuchi, M. & Lynd-Balta, E. (1995) *J. Neurosci.* **15**, 4851–4867.
41. Russchen, F. T., Amaral, D. G. & Price, J. L. (1987) *J. Comp. Neurol.* **256**, 175–210.
42. Ray, J. P. & Price, J. L. (1993) *J. Comp. Neurol.* **337**, 1–31.
43. Ferry, A. T., Öngür, D., An, X. & Price, J. L. (2000) *J. Comp. Neurol.* **425**, 447–470.
44. Öngür, D. & Price, J. L. (2000) *Cereb. Cortex* **10**, 206–219.
45. Bechara, A., Tranel, D., Damasio, H. & Damasio, A. R. (1996) *Cereb. Cortex* **6**, 215–225.
46. Bechara, A., Damasio, H., Tranel, D. & Damasio, A. R. (1997) *Science* **275**, 1293–1295.
47. Milne, E. & Grafman, J. (2001) *J. Neurosci.* **21**, 1–6.
48. Black, K. J. & Perlmutter, J. S. (1997) *Neuropsychiatry Neuropsychol. Behav. Neurol.* **10**, 147–150.
49. Saxena, S., Brody, A. L., Schwartz, J. M. & Baxter, L. R. (1998) *Br. J. Psychiatry* **35**, 26–36.
50. Willner, P. (1995) *Clin. Neuropharmacol.* **18**, S49–S56.
51. Tiihonen, J., Kuikka, J., Bergstrom, K., Lepola, U., Koponen, H. & Leinonen, E. (1997) *Am. J. Psychiatry* **154**, 239–242.
52. Shiba, M., Bower, J. H., Maraganore, D. M., McDonnell, S. K., Peterson, B. J., Ahlskog, J. E., Schaid, D. J. & Rocca, W. A. (2000) *Mov. Disord.* **15**, 669–677.
53. Mayberg, H. S., Liotti, M., Brannan, S. K., McGinnis, S., Mahurin, R. K., Jerabek, P. A., Silva, J. A., Tekell, J. L., Martin, C. C., Lancaster, J. L. & Fox, P. T. (1999) *Am. J. Psychiatry* **156**, 675–682.
54. Mayberg, H. S., Brannan, S. K., Tekell, J. L., Silva, J. A., Mahurin, R. K., McGinnis, S. & Jerabek, P. A. (2000) *Biol. Psychiatry* **48**, 830–843.
55. Liotti, M., Mayberg, H. S., Brannan, S. K., McGinnis, S., Jerabek, P. & Fox, P. T. (2000) *Biol. Psychiatry* **48**, 30–42.
56. Drevets, W. C., Price, J. L., Simpson, J. R., Jr., Todd, R. D., Reich, T., Vannier, M. & Raichle, M. E. (1997) *Nature* **386**, 824–827.
57. Öngür, D., Drevets, W. C. & Price, J. L. (1998) *Proc. Natl. Acad. Sci. USA* **95**, 13290–13295.
58. Van Hoesen, G. W., Morecraft, R. J. & Vogt, B. A. (1993) in *Neurobiology of Cingulate Cortex and Limbic Thalamus: A Comprehensive Handbook*, eds. Vogt, B. A. & Gabriel, M. (Birkhäuser, Boston), pp. 249–284.
59. Mega, M. S., Cummings, J. L., Salloway, S. & Malloy, P. (1997) *J. Neuro-psychiatr. Clin. Neurosci.* **9**, 315–330.
60. Drevets, W. C., Gautier, C., Price, J. C., Kupfer, D. J., Kinahan, P. E., Grace, A. A., Price, J. L. & Mathis, C. A. (2001) *Biol. Psychiatry* **49**, 81–96.
61. Piercey, M. F., Camacho-Ochoa, M. & Smith, M. W. (1995) *Clin. Neuropharmacol.* **18**, S34–S42.
62. Schwartz, W. J., Smith, C. B., Davidsen, L., Savaki, H. & Sokoloff, L. (1979) *Science* **205**, 723–725.
63. Ackermann, R. F., Finch, D. M., Babb, T. L. & Engel, J., Jr. (1984) *J. Neurosci.* **4**, 251–264.
64. Eidelberg, D., Moeller, J. R., Kazumata, K., Antonini, A., Sterio, D., Dhawan, V., Spetsieris, P., Alterman, R., Kelly, P. J., Dogali, M., Fazzini, E. & Beric, A. (1997) *Brain* **120**, 1315–1324.
65. Miller, R. D., ed. (1994) *Anesthesia* (Churchill Livingstone, New York).
66. Neumeyer, J. L., Lal, S. & Baldessarini, R. J. (1981) in *Apomorphine and Other Dopaminomimetics, Basic Pharmacology*, eds. Gessa, G. L. & Corsini, G. U. (Raven, New York), Vol. 1, pp. 1–17.
67. Andreu, N., Chale, J. J., Senard, J. M., Thalamas, C., Montastruc, J. L. & Rascol, O. (1999) *Clin. Neuropharmacol.* **22**, 15–23.
68. Parkinson Study Group (2000) *J. Am. Med. Assoc.* **284**, 1931–1938.
69. Magistretti, P. J. & Pellerin, L. (1999) *Philos. Trans. R. Soc. London B Biol. Sci.* **354**, 1155–1163.